

## Green-induced infrared absorption in MgO doped LiNbO<sub>3</sub>

Y. Furukawa<sup>a)</sup>

*OXIDE Corporation, 9633 Kobuchisawa, Kitakoma, Yamanashi 408-0044, Japan*

K. Kitamura

*National Institute for Research in Inorganic Materials, 1-1 Namiki, Tsukuba 305-0044, Japan*

A. Alexandrovski, R. K. Route, and M. M. Fejer

*E.L. Ginzton Laboratory, Stanford University, Stanford, California 94305*

G. Foulon

*Crystal Technology Inc., 1040 East Meadow Circle, Palo Alto, California 94303*

(Received 25 September 2000; accepted for publication 2 February 2001)

Green-induced infrared absorption (GRIIRA) was investigated by a photothermal technique for undoped and Mg-doped LiNbO<sub>3</sub> crystals that have different Li/Nb ratios. Threshold effect on GRIIRA was found, threshold MgO concentrations being the same for GRIIRA and photorefraction. We suggest that GRIIRA is associated with the formation of the small polaron that is located on Nb antisite defect. The remarkable decrease of GRIIRA in Mg:LiNbO<sub>3</sub> can then be attributed to the elimination of this intrinsic defect, Nb in Li, following the incorporation of Mg on Li sites. For nonlinear optical applications, LiNbO<sub>3</sub> doped with MgO at concentrations over threshold has a combined advantage of having almost no GRIIRA and photorefraction. © 2001 American Institute of Physics. [DOI: 10.1063/1.1359137]

In recent years there has been increasing interest in the use of quasi-phase-matched (QPM) nonlinear crystals<sup>1</sup> for a variety of frequency conversion applications. Periodically poled lithium niobate (PPLN) has been demonstrated to give efficient second-harmonic generation<sup>2</sup> and optical parametric oscillation<sup>3</sup> in both the cw and the Q-switched regimes. However, the performance of high power operating PPLN-SHG devices has been limited by material issues such as photorefractive beam distortion and green-induced infrared absorption (GRIIRA).<sup>4</sup> It has been demonstrated that the former problem can be solved by either high temperature device operation or MgO doping to the LiNbO<sub>3</sub> crystal, however, the latter problem still remains to be investigated. Defect models of the phenomena of green-induced infrared absorption have not been developed. Recently we reported that photorefraction in LiNbO<sub>3</sub> was completely eliminated by the doping of small amounts of MgO in crystals with near-stoichiometric composition.<sup>5</sup> These notable changes in material properties are strongly related to the elimination of Nb antisite defects (Nb<sub>Li</sub>) by the substitution of Mg on Li sites.

In this letter, we investigate the influence of MgO doping on the GRIIRA properties in LiNbO<sub>3</sub>, and demonstrate that LiNbO<sub>3</sub> crystals doped with MgO show remarkably lower GRIIRA than undoped LiNbO<sub>3</sub> crystals.

LiNbO<sub>3</sub> single crystals grown by two different methods were used in this study. They are denoted CLN when their stoichiometry, expressed as the ratio  $c_{\text{Li}} = [\text{Li}] / ([\text{Li}] + [\text{Nb}])$ , has a congruent-composition value of 48.4% and SLN when it deviates from this value in the direction of the stoichiometric composition of 50%. Crystals denoted as SLN and Mg:SLN were grown as described in earlier reports<sup>6</sup> by use of a top-seeded solution growth technique from a sto-

ichiometric melt with the addition of 11 mol % of K<sub>2</sub>O as flux and of MgO as dopant. Crystals denoted as CLN and Mg:CLN were grown by the conventional Czochralski method from congruent melt compositions. Chemical composition, Curie temperature, OH absorption wave number, and photorefractive damage threshold of the LiNbO<sub>3</sub> single crystals used in this study are summarized in Table I.<sup>7</sup> The corresponding chemical formulas were characterized by chemical analysis as follows: The crushed samples were dissolved with HNO<sub>3</sub>-HF solution in a closed Teflon vessel at 150 °C for one night. After being filtered for the separation of precipitated MgF<sub>2</sub>, the yielded solution was passed through as SA-a anion exchanger for further separation of Li and Nb ions. The Li and Mg content were analyzed by an inductively coupled plasma atomic emission spectrometry (ICP-AES). The Nb ions eliminated from the resin by HCl-HF solution were precipitated by cuperon, and the precipitate was dried and incinerated. The weight of the yielded Nb<sub>2</sub>O<sub>5</sub> gave the Nb content. The accuracy for [Li]/[Nb] cation ratios in Mg:SLN and Mg:CLN was 0.6% while that for MgO content amounted to 0.8%. As shown in Table I, it is clear that the SLN crystals contain lower intrinsic defect densities than conventional CLN crystals, but they still contain Nb<sub>Li</sub> at levels of thousands of ppm. On the other hand, extrinsic defects such as Fe were determined by ICP analysis to be in the ppm levels. In Table I, optical damage threshold refers to the onset of optical damage. The high MgO concentration samples, according to the data presented, displayed no optical damage, therefore the optical damage threshold was never reached. The high MgO concentration samples showed a shift in the OH absorption band from 3466 to 3485 to 3552 cm<sup>-1</sup> which suggests that at those doping levels, the excess Nb<sup>5+</sup> on Li sites has been completely replaced by Mg<sup>2+</sup>.<sup>5</sup>

<sup>a)</sup>Electronic mail: furukawa@opt-oxide.com

TABLE I. Chemical formula, Curie temperature, wave number of OH absorption, and photorefractive damage threshold of samples.

Sample	Chemical formula	Curie temperature (°C)	Position of OH absorption band (cm <sup>-1</sup> )	Optical damage threshold <sup>a</sup> (kW/cm <sup>2</sup> )
Nondoped CLN	Li <sub>0.950</sub> □ <sub>0.04</sub> Nb <sub>1.01</sub> O <sub>3</sub>	1145.0	3485	1
Mg30 CLN	Li <sub>0.925</sub> Mg <sub>0.030</sub> □ <sub>0.042</sub> Nb <sub>1.003</sub> O <sub>3</sub>	1188.5	3485	10
Mg45 CLN	Li <sub>0.901</sub> Mg <sub>0.045</sub> □ <sub>0.052</sub> Nb <sub>1.0018</sub> O <sub>3</sub>	1209.0	3485	75
Mg60 CLN	Li <sub>0.886</sub> Mg <sub>0.060</sub> □ <sub>0.055</sub> Nb <sub>0.9987</sub> O <sub>3</sub>	1220.0	3532	>8000 <sup>b</sup>
Nondoped SLN	Li <sub>0.990</sub> □ <sub>0.008</sub> Nb <sub>1.002</sub> O <sub>3</sub>	1192.0	3466	0.1
Mg06 SLN	Li <sub>0.9856</sub> Mg <sub>0.0072</sub> □ <sub>0.0066</sub> Nb <sub>1.0006</sub> O <sub>3</sub>	1205.5	3466	10
Mg18 SLN	Li <sub>0.972</sub> Mg <sub>0.019</sub> □ <sub>0.011</sub> Nb <sub>0.9980</sub> O <sub>3</sub>	1211.0	3532	>8000 <sup>b</sup>
Mg36 SLN	Li <sub>0.957</sub> Mg <sub>0.034</sub> □ <sub>0.014</sub> Nb <sub>0.9950</sub> O <sub>3</sub>	1210.5	3532	>8000 <sup>b</sup>

<sup>a</sup>Photorefractive damage threshold is defined as the cw green-light intensity where the transmitted laser beam is distorted as a result of photorefracton after 10 min of irradiation (see Ref. 5).

<sup>b</sup>No photorefracton was observed at this intensity level.

The technique for absorption measurement used in this work was photothermal common-path interferometry<sup>8</sup> which has the sensitivity of 0.1 ppm/cm. We measured absorption of an infrared pump beam (wavelength 1064 nm) with the power density of 21 kW/cm<sup>2</sup>, which was focused into 0.5 mm thick crystals. Both green and infrared light were propagated along the *z* axis in order to separate refractive index change caused by thermal effect from photorefractive effect. A green beam, with a wavelength of 532 nm and with the power density in the range 0.03–3.6 kW/cm<sup>2</sup>, was opened and closed manually. Green and IR beams were aligned to overlap inside the crystal so that the change of IR absorption in the presence of green light could be monitored. Values for photorefracton in the presence of green light were estimated under the same conditions as for the GRIIRA measurements. These values are estimated from the basic feature of the photothermal system, which detects any phase distortion of the probe beam caused by temperature change or photorefracton. Note that for the specific configuration used (light propagating along the optic axis, thin crystal) the observed index change is approximately two orders of magnitude lower than for the conventional geometry with extraordinary

polarized light propagating in the direction normal to the optic axis.

Figure 1 shows an example of green-induced infrared absorption and photorefracton as a function of time for an undoped, nearly stoichiometric LiNbO<sub>3</sub> crystal ([Li]/[Nb] = 0.988). As seen in this figure, undoped SLN shows small initial IR absorption (0.0017 cm<sup>-1</sup>) and a factor of five increase in IR absorption in the presence of green light. The green induced IR absorption observed here recovered to its original value when the green pump beam was turned off.

Figure 2 shows the effect of [Li]/[Nb] stoichiometry and Mg doping on the GRIIRA in LiNbO<sub>3</sub>. For low doping levels GRIIRA increased with the increase in Mg concentration, however, doping with Mg concentrations that exceeded certain threshold levels showed remarkable decreases of GRIIRA in both SLN and CLN cases. Mg:SLN requires a smaller Mg concentration than Mg:CLN for low GRIIRA state to be reached. The data plotted by open circles and open triangles in Fig. 2 show samples that exhibit no measurable photorefractive damage at 532 nm to intensities of as much as 8 MW/cm<sup>2</sup> in Table I.

Figure 3 shows photorefracton as a function of [Li]/

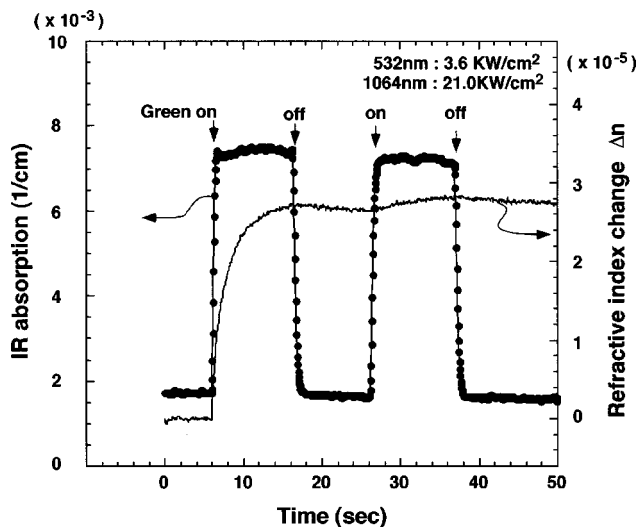


FIG. 1. Example of the change of infrared absorption and photorefracton by green light irradiation in an undoped nearly stoichiometric LiNbO<sub>3</sub> crystal listed in Table I.

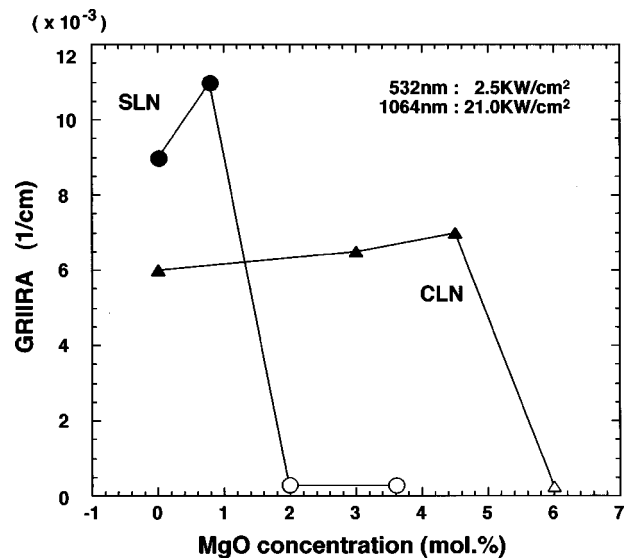


FIG. 2. Green induced infrared absorption (GRIIRA) vs MgO concentration in SLN and CLN crystals. Chemical formula and other material properties of these samples are listed in Table I.

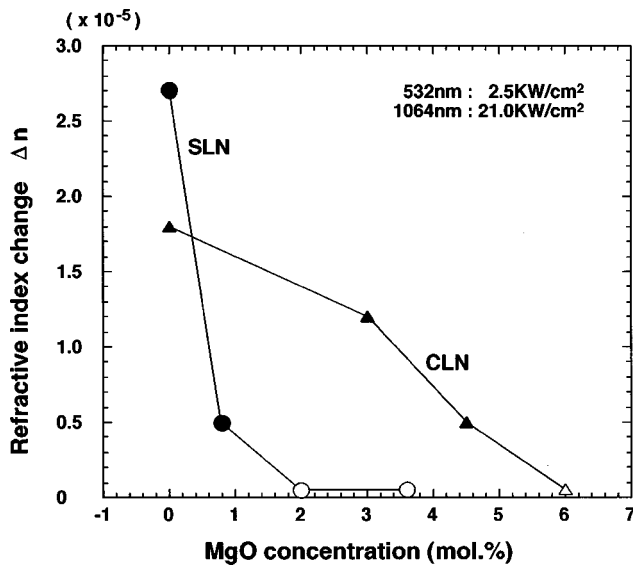


FIG. 3. Photorefractive index change vs MgO concentration in SLN and CLN crystals. Chemical formula and other material properties of these samples are listed in Table I.

[Nb] and MgO concentrations. The refractive index changes were measured along with the GRIIRA measurements shown in Fig. 2. The photorefractive index in both SLN and CLN crystals decreased monotonically with increase of MgO concentration. SLN crystals with high [Li]/[Nb] ratios show faster decreases of photorefractive index than congruent crystals. The feature similar to the GRIIRA behavior is the threshold doping level over which photorefractive index disappears along with the disappearance of GRIIRA.

The reasons for the threshold behavior of both photorefractive index and GRIIRA are probably related. Moreover, in Table I, the optical damage disappearance and the shift in the OH absorption band from 3466 to 3485 to 3532  $\text{cm}^{-1}$  both correspond to the same threshold MgO concentrations. The comparison with the chemical formulas strongly suggests that at these doping levels the excess  $\text{Nb}^{5+}$  on Li sites has been completely replaced by  $\text{Mg}^{2+}$ .<sup>5</sup>

We think that GRIIRA is associated with small polaron absorption band that is centered in the near IR, much like it occurs in reduced crystals though the absorption is several orders of magnitude less for crystals measured in this work. The small polaron is believed to be formed by electron trapped by antisite  $\text{Nb}$ .<sup>9,10</sup> The results of an early work<sup>11</sup> suggest that at room temperature that this trap is unstable, the decay time being in the range of milliseconds. This explains the rapid response of induced absorption on the green light power observed in Fig. 1. The significant decrease in GRIIRA over a threshold concentration can be attributed to the complete elimination of intrinsic defects of  $\text{Nb}_{\text{Li}}$  following the incorporation of Mg on Li sites.

The increase of GRIIRA with doping in the region under

threshold needs some comments. Both the rate of excitation of electrons to the conduction band and small polaron lifetime will contribute to the IR absorption along with  $\text{Nb}_{\text{Li}}$  concentration. As to the concentration, it is clear that undoped SLN crystals contain lower intrinsic defect densities than conventional CLN crystals, but they still contain  $\text{Nb}_{\text{Li}}$  at a level of thousands of ppm. Since SLN crystals show stronger GRIIRA than CLN crystals the other factors should play a very important role.

As for the excitation rate, it should be proportional to the concentration of the corresponding defects responsible for the green absorption. Fe impurity is known to contribute to excitation of electrons to the conduction band. The concentration of Fe was determined by chemical (ICP) analysis to be in the ppm levels both in SLN and CLN. This number is well below the concentration of  $\text{Nb}_{\text{Li}}$  shallow traps, even in SLN, so that it is likely that most excited electrons will be trapped by  $\text{Nb}_{\text{Li}}$ . This is why the dominant factor in GRIIRA, for the same excitation rate, is probably small polaron lifetime. In this way it is possible that small polaron lifetime increases dramatically near the threshold. This assumption has to be checked experimentally.

In summary, we have investigated green-induced infrared absorption and photorefractive index by means of the photo-thermal common-path interferometry technique. We observed that MgO doping had similar results for reducing GRIIRA in  $\text{LiNbO}_3$ , namely that less MgO was necessary to eliminate GRIIRA in stoichiometric  $\text{LiNbO}_3$  than in congruent  $\text{LiNbO}_3$ .  $\text{LiNbO}_3$  crystals doped with MgO at levels exceeding threshold concentrations of 1 mol. % for SLN and 5 mol. % for CLN exhibit no measurable GRIIRA with an irradiation up to 3.5  $\text{kW}/\text{cm}^2$  of green light. This remarkable decrease of GRIIRA in  $\text{Mg}:\text{LiNbO}_3$  is attributed to the elimination of antisite intrinsic defects of  $\text{Nb}_{\text{Li}}$ .

<sup>1</sup>M. M. Fejer, G. A. Magel, D. H. Jundt, and R. L. Byer, *IEEE J. Quantum Electron.* **QE-28**, 2631 (1992).

<sup>2</sup>K. Mizuuchi, K. Yamamoto, and M. Kato, *Electron. Lett.* **25**, 731 (1997).

<sup>3</sup>L. E. Myers, G. D. Miller, R. C. Eckardt, M. M. Fejer, R. L. Byer, and W. R. Bosenberg, *Opt. Lett.* **20**, 52 (1995).

<sup>4</sup>R. G. Batchko, G. D. Miller, A. Alexandrovski, M. M. Fejer, and R. L. Byer, *1998 OSA Technical Digest Series* (Optical Society of America, Washington, DC, 1998), Vol. 12, pp. 75–76.

<sup>5</sup>Y. Furukawa, K. Kitamura, S. Takekawa, K. Niwa, and H. Hatano, *Opt. Lett.* **23**, 1892 (1998).

<sup>6</sup>K. Niwa, Y. Furukawa, K. Kitamura, S. Takekawa, and H. Hatano, *J. Cryst. Growth* **208**, 493 (2000).

<sup>7</sup>Y. Furukawa, K. Kitamura, S. Takekawa, K. Niwa, Y. Yajima, N. Iyi, I. Mnushkina, P. Guggenheim, and J. Martin, *J. Cryst. Growth* **211**, 230 (2000).

<sup>8</sup>A. Alexandrovski, G. Foulon, L. E. Myers, R. K. Route, and M. M. Fejer, *Proc. SPIE* **3610**, 44 (1999).

<sup>9</sup>K. Buse, F. Jermann, and E. Krätzig, *Opt. Mater.* **4**, 237 (1995).

<sup>10</sup>F. Jermann, M. Simon, and E. Krätzig, *J. Opt. Soc. Am. B* **12**, 2066 (1995).

<sup>11</sup>E. G. Valyashko and V. A. Timoshenkov, *Zh. Prikl. Spektrosk.* **15**, 1008 (1971).